Table 3 The $\overline{Nu}_L Gr_L^{*-1/5}$ results for power law variation of the surface heat flux

ξ_L	Pr = 0.1			Pr = 0.7			Pr = 7			Pr = 100		
	n			n			n			n		
	−0.5	0	0.5	−0.5	0	0.5	−0.5	0	0.5	−0.5	0	0.5
0	0.3818	0.4543	0.4678	0.7239	0.8338	0.8457	1.339	1.500	1.505	2.417	2.6814	2.6810
0.5	0.4710	0.5637	0.6039	0.8162	0.9466	0.9983	1.436	1.617	1.683	2.515	2.801	2.896
1.0	0.7218	0.8494	0.8805	1.081	1.252	1.288	1.714	1.936	1.966	2.797	3.125	3.154
1.5	1.141	1.297	1.328	1.490	1.706	1.753	2.140	2.403	2.439	3.244	3.634	3.678
2.0	1.794	1.926	1.940	2.026	2.279	2.334	2.691	3.063	3.123	3.828	4.286	4.347
2.5	2.649	2.724	2.715	2.688	2.979	3.032	3.366	3.816	3.890	4.516	5.042	5.120
3.0	3.654	3.677	3.645	3.544	3.833	3.870	4.157	4.634	4.718	5.335	5.961	6.054
3.5	4.796	4.778	4.727	4.646	4.868	4.874	5.035	5.538	5.635	6.305	7.011	7.137
4.0	6.075	6.027	5.961	5.953	6.077	6.054	6.008	6.569	6.677	7.373	8.163	8.293
4.5	7.499	7.430	7.355	7.409	7.459	7.414	7.198	7.786	7.887	8.562	9.431	9.609
5.0	9.080	9.000	8.924	9.015	9.018	8.963	8.696	9.226	9.308	9.859	10.850	11.046

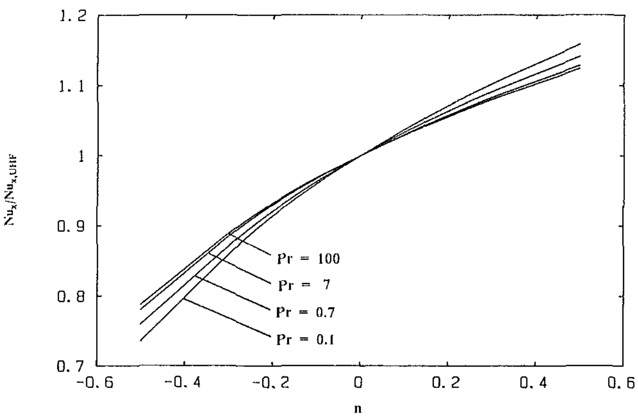

Fig. 2 $Nu_x/Nu_{x,UHF}$ versus n for flat plates ($\Lambda = 0$)

$$\mathrm{Nu}_x \mathrm{Gr}_x^{*-1/5} = \alpha(\mathrm{Pr})[A(\Lambda) + f_1(\mathrm{Pr})\Lambda](1 + VW) \quad (17)$$

where

$$\alpha(\mathrm{Pr}) = \mathrm{Pr}^{2/5}(4 + 9\mathrm{Pr}^{1/2} + 10\mathrm{Pr})^{-1/5} \quad (18a)$$

$$A(\Lambda) = 1 + 0.09\Lambda^{1/2} \quad (18b)$$

$$f_1(\mathrm{Pr}) = (0.032 + 0.176\mathrm{Pr}^{-0.384}) \quad (18c)$$

$$V = \{[0.328 + 0.343 \exp(-2.12\mathrm{Pr}^{1/5})] - 0.195n\}n \quad (18d)$$

$$W = \exp[-(0.0265 + 0.0907\mathrm{Pr}^{-0.444})\Lambda^{0.8}] \quad (18e)$$

The average Nusselt number for the same ranges of parametric values can be correlated by

$$\overline{\mathrm{Nu}}_L \mathrm{Gr}_L^{*-1/5} = \frac{5}{4}\alpha(\mathrm{Pr})\ [B(\Lambda) + f_2(\mathrm{Pr})\Lambda](1 + \bar{V}) \quad (19)$$

where

$$B(\Lambda) = 1 + 0.08\Lambda^{1/2} \quad (20a)$$

$$f_2(\mathrm{Pr}) = (0.026 + 0.14\mathrm{Pr}^{-0.39}) \quad (20b)$$

$$\bar{V} = (4VW - n\bar{W})/(4 + n\bar{W}) \quad (20c)$$

$$\bar{W} = \exp(-0.5\Lambda^{0.6}) \quad (20d)$$

with Λ in equations (19) and (20) now standing for Λ_L or Λ at $x = L$.

It is interesting to note that for the UHF case ($n = 0$) V and $\bar{V}$ in equations (17) and (19) become zero. It is also interesting to note that for the flat plate (i.e., $\Lambda = 0$) the terms $[A(\Lambda) + f_1(\mathrm{Pr})\Lambda]$ and $[B(\Lambda) + f_2(\mathrm{Pr})\Lambda]$ both become one. Therefore, for the flat plate solution under UHF, $\mathrm{Nu}_x \mathrm{Gr}_x^{*-1/5} = \alpha(\mathrm{Pr})$, where $\alpha(\mathrm{Pr})$ is taken from Fujii and Fujii (1976). The maximum error in the correlations for the local and average Nusselt numbers is less than 5 percent for the UHF case and less than 8.3 percent for the variable heat flux condition.

References

Elenbaas, W., 1948, "The Dissipation of Heat by Free Convection From Vertical and Horizontal Cylinders," *Journal of Applied Physics*, Vol. 19, pp. 1148–1154.

Fujii, T., and Fujii, M., 1976, "The Dependence of Local Nusselt Number in the Case of Free Convection Along a Vertical Surface With Uniform Heat Flux," *International Journal of Heat and Mass Transfer*, Vol. 19, pp. 121–122.

Fujii, T., and Uehara, H., 1970, "Laminar Natural Convective Heat Transfer From the Outer Surface of a Vertical Cylinder," *International Journal of Heat and Mass Transfer*, Vol. 13, pp. 607–615.

Gebhart, B., 1971, *Heat Transfer*, 2nd ed., McGraw-Hill, New York, p. 340.

Kuiken, H. K., 1968, "Axisymmetric Free Convection Boundary Layer Flow Past Slender Bodies," *International Journal of Heat and Mass Transfer*, Vol. 11, pp. 1141–1153.

Kuiken, H. K., 1974, "The Thick Free-Convective Boundary-Layer Along a Semi-infinite Isothermal Vertical Cylinder," *Journal of Applied Mathematics and Physics* (ZAMP), Vol. 25, pp. 497–514.

Lee, H. R., Chen, T. S., and Armaly, B. F., 1988, "Natural Convection Along Vertical Cylinders With Variable Surface Temperature," ASME Journal of Heat Transfer, Vol. 110, pp. 103–108.

Lee, S. L., Chen, T. S., and Armaly, B. F., 1986a, "Mixed Convection Along Isothermal Vertical Cylinders and Needles," *Proceedings of the Eighth International Heat Transfer Conference*, Vol. 3, pp. 1425–1432.

Lee, S. L., Chen, T. S., and Armaly, B. F., 1986b, "New Finite Difference Solution Methods for Wave Instability Problems," *Numerical Heat Transfer*, Vol. 10, pp. 1–8.

Lee, S. L., Chen, T. S., and Armaly, B. F., 1987, "Mixed Convection Along Vertical Cylinders and Needles With Uniform Surface Heat Flux," ASME Journal of Heat Transfer, Vol. 109, pp. 711–716.

Minkowycz, W. J., and Sparrow, E. M., 1974, "Local Nonsimilar Solutions for Natural Convection on a Vertical Cylinder," ASME Journal of Heat Transfer, Vol. 96, pp. 178–183.

Sparrow, E. M., and Gregg, J. L., 1956, "Laminar-Free-Convection Heat Transfer From the Outer Surface of a Vertical Circular Cylinder," *Transactions ASME*, Vol. 78, pp. 1823–1829.

A General Correlation for Melting in Rectangular Enclosures

C. Beckermann[1]

Introduction

The problem of melting of ordinary (nonmetallic) and metallic solids in enclosures has received considerable research attention due to its importance, for example, in materials pro-

[1] Department of Mechanical Engineering, The University of Iowa, Iowa City, IA 52242.

Contributed by the Heat Transfer Division for publication in the Journal of Heat Transfer. Manuscript received by the Heat Transfer Division September 13, 1988. Keywords: Modeling and Scaling, Natural Convection, Phase-Change Phenomena.

cessing and latent heat energy storage. It is well known that natural convection in the melt, as well as heat conduction in the solid, considerably influence the solid/liquid interface shape and motion. However, attempts to correlate the average heat transfer and melting rates have been relatively unsuccessful, except for a few special cases (Viskanta, 1985).

Many experimental and numerical studies of melting with natural convection have shown that three distinctive heat transfer regimes can be identified (Viskanta, 1985): (1) an initial regime during which the heat transfer in the small melt layer is by pure conduction, (2) a transition regime characterized by developing natural convection in the melt, and (3) a quasi-steady natural convection regime during which the heat transfer rate across the melt region is approximately constant. The above scenario of the heat transfer processes across the melt holds for a large range of Rayleigh (Ra), Stefan (Ste), and Prandtl (Pr) numbers, as well as for a variety of geometries. Recently, it has been shown that the above regimes also exist during melting with heat conduction in the solid (Benard et al., 1986; Beckermann and Viskanta, 1989).

Despite a good understanding of the physical phenomena occurring during melting in enclosures, it has not been possible to correlate the melting rates and heat transfer data of various independent investigators accurately (Viskanta, 1985). For the case of melting from a vertical wall of a solid that is at the fusion temperature, Webb and Viskanta (1985) concluded that conventional correlation techniques fail to collapse the data, because the length scale in the governing dimensionless parameters changes with time as the size of the melt region increases. Through a careful scaling analysis, Jany and Bejan (1988) were able to construct heat transfer and melt fraction correlations that cover the entire time domain. Their investigation is, however, limited to melting from a heated vertical wall inside cavities with the solid at the fusion temperature and laminar natural convection in the melt. No attempt is made to generalize these results for other initial and boundary conditions. For example, they conclude "if one is to consider the additional effect of [heat] conduction in the solid, one must construct a new scenario . . . It is not a question of merely introducing a new dimensionless group . . .".

Consequently, the objective of this study is to demonstrate that a more general melt fraction correlation can be obtained covering the entire time domain as well as the additional effect of heat conduction in the solid. The present analysis is based on the assumptions that (1) the melting proceeds through the three heat transfer regimes described above and (2) the liquid and solid Stefan numbers are small so that the heat transfer is quasi-steady (i.e., negligible thermal inertia of the liquid and solid). The latter assumption is supported by the fact that in virtually all previous numerical and experimental studies the Stefan numbers were less than about 0.3 (Webb and Viskanta, 1985; Viskanta, 1985; Benard et al., 1986). For conciseness, this study concentrates on melting in rectangular enclosures. However, the methods presented can easily be applied to other geometries (e.g., cylinders, etc.). The melt fraction correlation derived in this study is validated using the example of melting of metals in vertical cavities.

Analysis

The physical system considered in the present study consists of a rectangular enclosure with two vertical side walls of height H held at uniform temperatures and the connecting walls of length L well insulated. Initially, the enclosure is filled with a solid of fusion temperature T_f. Melting is initiated by raising the left ("hot") wall temperature to $T_H > T_f$, while maintaining the right ("cold") wall at $T_C \leq T_f$. The assumption of quasi-steady heat transfer in the liquid and solid regions (see the Introduction) implies that the difference between the heat transfer rates supplied through the hot wall and extracted through the cold wall is exclusively used to advance the melting front. In other words, the thermal inertia of the system is assumed to be negligibly small, so that the mean temperatures of the liquid and solid are constant. Again, this assumption is good in the limit of small Stefan numbers. An overall energy balance on the enclosure can now be written, in dimensionless form, as

$$\overline{\mathrm{Nu}}_H - \overline{\mathrm{Nu}}_C = \frac{d\bar{s}}{d\tau} \qquad (1)$$

The use of the average melt region width $\bar{s}$ is preferable over the melt fraction f, because it eliminates the aspect ratio A as a parameter in equation (1). The two quantities $\bar{s}$ and f are related by

$$f = \frac{1}{HL}\int_0^H S dy = \bar{s}A \qquad (2)$$

where $A = H/L$, S is the local melt region width, and y is the vertical coordinate. The other dimensionless quantities in equation (1) are defined as

$$\tau = \frac{c_l(T_H - T_f)}{\Delta h_f}\,\frac{t\alpha_l}{H^2}\,\frac{\rho_l}{\rho_s} = \mathrm{Ste\ Fo}/\rho^*$$

dimensionless time

$$\overline{\mathrm{Nu}}_H = \frac{\overline{q''_H}H}{(T_H - T_f)k_l}$$

average Nusselt number at the hot wall (3)

$$\overline{\mathrm{Nu}}_C = \frac{\overline{q''_C}H}{(T_H - T_f)k_l}$$

average Nusselt number at the cold wall

where k, c, ρ, α, $\overline{q''}$, t, and Δh_f are the thermal conductivity, specific heat, density, thermal diffusivity, average heat flux, time, and latent heat of fusion, respectively, while the subscripts l and s denote the liquid and solid phases, respectively. According to the above definitions, the average Nusselt numbers at the hot and cold walls will be equal at steady state. Furthermore, it is evident that equation (1) can also be derived by integrating a local interfacial energy balance over the height of the enclosure and relating the heat transfer rates on both sides of the solid/liquid interface to the heat transfer rates at the hot and cold walls.

The fact that equation (1) is valid regardless of the particular physical situation considered (i.e., Ra, Pr, orientation of the enclosure, etc.), together with the fact that virtually all melting processes are characterized by the three heat transfer regimes outlined in the Introduction, holds the key for obtaining a general correlation for the melt fraction (i.e., $\bar{s}$). Because the Nusselt numbers are not constant, equation (1) cannot be integrated over the entire time domain. For the case of $\overline{\mathrm{Nu}}_C = 0$ (no heat conduction in the solid), a number of investigators have integrated equation (1) by using separate $\overline{\mathrm{Nu}}_H$ relations for the various heat transfer regimes (Webb and Viskanta, 1985; Benard et al., 1985; Jany and Bejan, 1988; and others). Through comparisons with experiments and numerical simulations, these studies have shown that accurate melt fraction correlations can be obtained by simply matching the solutions for the first conduction regime and the third quasi-steady natural convection regime. This approach is followed in the present study.

Conduction Regime. In the initial conduction regime, the solid/liquid interface is planar and parallel to the hot wall, so that the heat transfer through the liquid and solid regions is one dimensional. Consequently, the Nusselt numbers for regime 1 can be expressed as

$$\overline{\mathrm{Nu}}_{H,1}=\frac{1}{\bar{s}} \qquad \overline{\mathrm{Nu}}_{C,1}=\frac{\Phi}{1-\bar{s}} \tag{4}$$

where the subcooling parameter Φ is defined as $\Phi=(T_f-T_C)k_s/(T_H-T_f)k_l$. Equation (1) can now be written as

$$\frac{1}{\bar{s}}-\frac{\Phi}{1-\bar{s}}=\frac{d\bar{s}}{d\tau} \tag{5}$$

With $\bar{s}(\tau=0)=0$, the solution to equation (5) is given by

$$\tau=\bar{s}\bar{s}_c-\bar{s}_c^2\ln(1-\bar{s}/\bar{s}_c)+\bar{s}_c^3[1.5+0.5(1-\bar{s}/\bar{s}_c)^2 - 2(1-\bar{s}/\bar{s}_c)+\ln(1-\bar{s}/\bar{s}_c)] \tag{6}$$

where $\bar{s}_c$ is the average melt region width at steady state, if the entire melting process were conduction dominated, and is given by

$$\bar{s}_c=\frac{1}{1+\Phi} \tag{7}$$

It can immediately be seen that for the case of $\Phi=0$ (i.e., no heat conduction in the solid, equation (6) reduces to $\bar{s}=(2\tau)^{1/2}$, which is nothing else but Neumann's solution in the limit of Ste$\to 0$. It is interesting to note that for Ste$=0.1$, the constant $2^{1/2}$ is only 1.6 percent higher than for Ste$\to 0$. For Ste$=0.3$, the difference increases to 4.6 percent. Virtually all previous studies of melting in enclosures have been performed for Ste<0.3 (Webb and Viskanta, 1985).

Following the procedure proposed by Benard et al. (1985), the conduction regime ends at the time τ_o when $\overline{\mathrm{Nu}}_{H,1}$ is equal to $\overline{\mathrm{Nu}}_{H,3}$, the average Nusselt number at the hot wall during the third quasi-steady convection regime. Consequently, the time τ_o can be calculated by substituting $\bar{s}_o=1/\overline{\mathrm{Nu}}_{H,3}$ into equation (6).

Convection Regime. In the third quasi-steady natural convection regime, the solid/liquid interface is no longer planar, so that the heat transfer by conduction through the solid region is two (or three) dimensional. In the present study, the average Nusselt number at the cold wall during the third regime is approximated by

$$\overline{\mathrm{Nu}}_{C,3}=\frac{c\Phi}{1-\bar{s}} \tag{8}$$

where c is not necessarily constant since the shape of the solid region can vary continuously. It will be shown, however, that for a reasonably wide range of the governing parameters, c can be taken as constant, if c is determined through appropriate comparisons with experiments or numerical simulations.

For the convection regime, equation (1) can now be rewritten as

$$\overline{\mathrm{Nu}}_{H,3}-\frac{c\Phi}{1-\bar{s}}=\frac{d\bar{s}}{d\tau} \tag{9}$$

Note that $\overline{\mathrm{Nu}}_{H,3}$ is constant throughout the quasi-steady natural convection regime, as has been established by many researchers for a large variety of physical situations (Viskanta, 1985). With the initial condition $\bar{s}(\tau_o)=\bar{s}_o=1/\overline{\mathrm{Nu}}_{H,3}$, equation (9) can be integrated to yield

$$(\bar{s}-\bar{s}_o)-(1-\bar{s}_f)\ln\left(\frac{\bar{s}-\bar{s}_f}{\bar{s}_o-\bar{s}_f}\right)=\overline{\mathrm{Nu}}_{H,3}(\tau-\tau_o) \tag{10}$$

where $\bar{s}_f$ is the (final) average melt region width when melting ends, and is given by

$$\bar{s}_f=1-\frac{c\Phi}{\overline{\mathrm{Nu}}_{H,3}} \tag{11}$$

Note that according to equation (11) and with the knowledge of $\overline{\mathrm{Nu}}_{H,3}$ (see below), the constant c can be directly determined from final melt fraction data. Again, in the case of $\Phi=0$ (i.e., no heat conduction in the solid), equation (10) reduces to $\bar{s}-\bar{s}_o=\overline{\mathrm{Nu}}_{H,3}\ (\tau-\tau_o)$. This linear variation of the melt fraction (i.e., $\bar{s}$) with time is well known for melting of a solid at its fusion temperature during the quasi-steady convection regime (Webb and Viskanta, 1985; Benard et al., 1985; Jany and Bejan, 1988). For the case of $\Phi=0$, an additional regime can be identified after part of the solid/liquid interface reaches the right ("cold") wall. This fourth "shrinking solid" (Jany and Bejan, 1988) regime has been considered in detail in other studies (Benard et al., 1985). Also, note that $\Phi=0$ not only implies that $T_C=T_f$, but that the entire solid is isothermally at the fusion temperature and, according to equations (4) and (8), that the Nusselt number at the cold wall is equal to zero. Consequently, the case of $\Phi=0$ applies to both, enclosures with $T_C=T_f$ and enclosures with an adiabatic right ("cold") wall.

For the case of $\Phi=0$, Jany and Bejan (1988) proposed to match the melt fraction (i.e., $\bar{s}$) correlations for the conduction and convection regimes by combining them in a canonical relationship. The results of Benard et al. (1985), as well as the present comparisons (see below) indicate, however, that this is not necessary, because at τ_o equations (6) and (10) match relatively smoothly.

Nusselt Number Correlations. By specifying $\overline{\mathrm{Nu}}_{H,3}$, the general melt fraction (i.e., $\bar{s}$) correlation, equations (6) and (10), can be adapted to a particular physical situation. Theoretically, $\overline{\mathrm{Nu}}_{H,3}$ is a function of the size and shape of the melt region, the orientation of the enclosure, and the Rayleigh and Prandtl numbers. It is known, however, that most correlations for natural convection in rectangular enclosures also work if the enclosure has curved surfaces (Lienhard, 1973). This has prompted many researchers to calculate $\overline{\mathrm{Nu}}_{H,3}$ from standard correlations for steady natural convection in rectangular enclosures without phase change. The validity of the above approach has been demonstrated for a large variety of physical systems, including melting of paraffins and metals from the side without heat conduction in the solid (Benard et al., 1985; Viskanta, 1985; Webb and Viskanta, 1986a; Jany and Bejan, 1988), with heat conduction in the solid (Benard et al., 1986; Beckermann and Viskanta, 1989), as well as melting from below (Gau and Viskanta, 1986). Some investigators (Hale and Viskanta, 1980; Webb and Viskanta, 1986b) have calculated the Rayleigh number in such standard Nusselt number correlations by choosing the instantaneous average melt region width $\bar{s}$ as the characteristic length scale, instead of H. This results, however, in a continuously varying Nusselt number and contradicts the observed quasi-steady heat transfer behavior during the third regime. Furthermore, it is known that for vertical enclosures, the aspect ratio has only a minor effect on the Nusselt number, if the vertical dimension (i.e., H) is used as the characteristic length scale (Jany and Bejan, 1988).

A number of investigators have measured quasi-steady Nusselt numbers directly, under melting conditions (Viskanta, 1985). Interestingly, it has been found that a single $\overline{\mathrm{Nu}}_{H,3}$ correlation can be used for melting of a paraffin ($\mathrm{Pr}\approx 50$) inside a vertical cavity, regardless of whether there is heat conduction in the solid or not (Benard et al., 1985, 1986). Unfortunately, Benard et al. (1986) do not provide any melt fraction data for their experiment with $\Phi=5.952$, so that the present melt fraction correlation cannot be tested for $\mathrm{Pr}>1$ and $\Phi\neq 0$. Furthermore, the $\overline{\mathrm{Nu}}_{H,3}$ correlation by Benard et al. (1985, 1986) is in close agreement with standard Nusselt number correlations for steady natural convection in vertical cavities without phase change, indicating that such standard correlations can generally be used to calculate $\overline{\mathrm{Nu}}_H$ during the third regime.

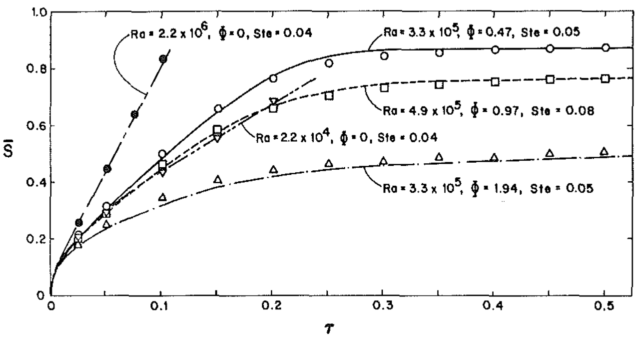

Fig. 1 Comparison of the melt fraction correlation (lines) with previous numerical data (● and ▿: Webb and Viskanta, 1986a; ○, □, and △: Beckermann and Viskanta, 1988) for melting of gallium (Pr = 0.021) inside a vertical cavity

Example: Melting of Metals in Vertical Cavities

For the case of melting of metals with heat conduction in the solid inside a vertical rectangular enclosure, Beckermann and Viskanta (1989) obtained the following $\overline{\mathrm{Nu}}_{H,3}$ correlation:

$$\overline{Nu}_{H,3} = 0.5(\mathrm{RaPr})^{0.25} \tag{12}$$

The validity of the above correlation was tested for $10^4 < \mathrm{Ra} < 10^6$, $\mathrm{Pr} < 1$, $0.01 < \mathrm{Ste} < 0.09$, and $\Phi < 2.5$. Equation (12) is in good agreement with a similar correlation obtained by Webb and Viskanta (1986a) for melting of gallium without heat conduction in the solid, as well as with Nusselt number data for steady natural convection (i.e., without melting) of tin and gallium in a vertical square enclosure (Wolff et al., 1988). These observations further support the simple treatment of the third regime proposed in the present study (see also the section Nusselt Number Correlations).

Figure 1 shows a comparison of the present melt fraction (i.e., $\bar{s}$) correlation with numerical data obtained by Webb and Viskanta (1989) (● and ▿) and Beckermann and Viskanta (1989) (○, □, and △) for melting of gallium ($\mathrm{Pr} = 0.021$) inside vertical rectangular enclosures. It should be noted that the numerical results of the above two investigations were verified experimentally. The constant c in equation (11) was determined by Beckermann and Viskanta (1989), who found that with $c = 1.19$, equation (11) correlates the final melt fraction data (i.e., at steady state) to within 3 percent. It can be seen from Fig. 1 that the present melt fraction (i.e., $\bar{s}$) correlation (lines) fits the numerical results (symbols) very well. Slightly better agreement could have been obtained by using the numerically determined Nusselt numbers in the melt fraction correlation, instead of calculating them from equation (12). For the three cases with heat conduction in the solid, some disagreement is due to inaccuracies in the constant c ($= 1.19$). As discussed earlier, c varies slightly during the third regime, because of variations in the shape of the solid region. It should also be noted that the numerical simulations for the case of no heat conduction in the solid ($\Phi = 0$) were terminated before the solid/liquid interface reaches the right ("cold") wall (Webb and Viskanta, 1986a). This time instant also marks the end of the validity of the present melt fraction correlation. For $\Phi \neq 0$, the interface does not come into contact with the cold wall, so that the present correlation works throughout the entire time domain.

Conclusions

A model has been presented for melting in rectangular enclosures with natural convection in the melt and heat conduction in the solid. By assuming negligible thermal inertia in the liquid and solid regions, and dividing the time domain into three heat transfer regimes, the model equation has been integrated to yield simple algebraic expressions for the time variation of the melt fraction. The expressions are independent of the dimensionless parameters of the problem and can, therefore, be applied to any situation involving melting in differentially heated rectangular enclosures. The present melt fraction correlation can be adapted to a particular physical system by specifying the average Nusselt number at the hot wall during the third, quasi-steady convection regime. Such Nusselt numbers can generally be obtained from standard correlations for pure natural convection (i.e., without melting). As opposed to previous correlations, the present melt fraction correlation is equally valid for melting with and without heat conduction in the solid region.

The usefulness and accuracy of the proposed melt fraction correlation have been demonstrated for melting of metals in vertical cavities. The correlation is found to agree to within a few percent with melt fraction data from previous two-dimensional numerical simulations. Therefore, this correlation represents the first one to predict the time variation of the melt fraction realistically during melting with natural convection in the melt and heat conduction in the solid.

It is expected that the general melt fraction correlation derived in this study can equally well be applied to other configurations. Correlations, similar to the present one in the limiting case of *no* heat conduction in the solid, have been found to work well, for example, for melting of paraffins at their fusion temperature inside vertical (Benard et al., 1985) inclined (Webb and Viskanta, 1986b), and horizontal (Hale and Viskanta, 1980) rectangular enclosures. Since Nusselt number correlations are available for these configurations, extension to melting *with* heat conduction in the solid would require determination of the constant c only (from final melt fraction data). However, the lack of melt fraction data for the case of melting with heat conduction in the solid makes a definite test of the present melt fraction correlation for other configurations impossible.

It is possible to extend the present analysis to large Stefan numbers (i.e., large thermal inertia of the liquid and solid regions). For the case of $\Phi = 0$, Jany and Bejan (1988) proposed a simple procedure for correlating the melting rate for large liquid thermal inertia [i.e., the Nusselt numbers are reduced by a factor of the order of $1/(1+\mathrm{Ste})$]. This procedure could easily be adapted to the present case of melting with heat conduction in the solid (i.e., $\Phi \neq 0$).

Finally, it should be mentioned that the present correlation is not directly applicable to solidification, because the heat transfer across the liquid does not proceed through the same three regimes as in melting and, in addition, may not be quasi-steady. While some of the basic methods presented in this study may be utilized, correlation of solid fraction data for solidification represents a major challenge for future research.

Acknowledgments

The work reported in this paper was supported, in part, by the National Science Foundation under Grant No. CBT8808888 and through The University of Iowa Old Gold Summer Fellowship.

References

Beckermann, C., and Viskanta, R., 1989, "Effect of Solid Subcooling on Natural Convection Melting of a Pure Metal," ASME JOURNAL OF HEAT TRANSFER, Vol. *111*, pp. 416–424.

Benard, C., Gobin, D., and Martinez, F., 1985, "Melting in Rectangular Enclosures: Experiments and Numerical Simulations," ASME JOURNAL OF HEAT TRANSFER, Vol. 107, pp. 794–803.

Benard, C., Gobin, D., and Zanoli, A., 1986, "Moving Boundary Problem: Heat Conduction in the Solid Phase of a Phase-Change Material During Melting Driven by Natural Convection in the Liquid," *International Journal of Heat and Mass Transfer*, Vol. 29, pp. 1669–1681.

Gau, C., and Viskanta, R., 1986, "Melting and Solidification of a Pure Metal on a Vertical Wall," ASME JOURNAL OF HEAT TRANSFER, Vol. 108, pp. 174–181.

Hale, N. W., and Viskanta, R., 1980, "Solid-Liquid Phase-Change Heat Transfer and Interface Motion in Materials Cooled or Heated From Above or Below," *International Journal of Heat and Mass Transfer*, Vol. 23, pp. 283-292.

Jany, P., and Bejan, A., 1988, "Scaling Theory of Melting With Natural Convection in an Enclosure," *International Journal of Heat and Mass Transfer*, Vol. 31, pp. 1221-1235.

Lienhard, J. H., 1973, "On the Commonality of Equations for Natural Convection From Immersed Bodies," *International Journal of Heat and Mass Transfer*, Vol. 16, pp. 2121-2123.

Viskanta, R., 1985, "Natural Convection in Melting and Solidification," in: *Natural Convection: Fundamentals and Applications*, S. Kakac et al., eds., Hemisphere, Washington, DC, pp. 845-877.

Webb, B. W., and Viskanta, R., 1985, "On the Characteristic Length Scale for Correlating Melting Heat Transfer Data," *Int. Comm. Heat Mass Transfer*, Vol. 12, pp. 637-646.

Webb, B. W., and Viskanta, R., 1986a, "Analysis of Heat Transfer During Melting of a Pure Metal From an Isothermal Vertical Wall," *Numerical Heat Transfer*, Vol. 5, pp. 539-558.

Webb, B. W., and Viskanta, R., 1986b, "Natural-Convection-Dominated Melting Heat Transfer in an Inclined Rectangular Enclosure," *International Journal of Heat and Mass Transfer*, Vol. 29, pp. 183-192.

Wolff, F., Beckermann, C., and Viskanta, R., 1988, "Natural Convection of Liquid Metals in Vertical Cavities," *Experimental Thermal and Fluid Science*, Vol. 1, pp. 83-91.

Radiation View Factors From a Finite Rectangular Plate

B. T. F. Chung[1] and M. M. Kermani[2]

Introduction

The determination of radiation view factors from a differential strip to a rectangular plate, or in more general cases, radiation from a rectangular plate to other finite geometries, has practical importance in many engineering applications. Examples are radiation exchange within the internal engine cavities of gas turbines, furnaces, kilns, reactors, and other devices that normally operate at high temperatures. Hamilton and Morgan (1952) determined view factors analytically for several cases regarding a differential element and a differential strip to a plate. Their formulations are restricted to special conditions in that the elements under consideration are in a particular orientation and location with respect to the plate. Other formulations reported by Hottel and Sarofim (1967), Sparrow and Cess (1978), and Siegel and Howell (1981) also apply to special cases in that either the surface under consideration (plate, differential strip, or cylinder) is infinitely long, or there are two planar surfaces that share a common edge. To date, the general analytical expression for view factor from a rectangular plate with an arbitrary orientation and dimensions has not been available.

This study attempts to develop an exact and general formula for shape factors: (1) from a differential element to an arbitrary nonintersecting finite rectangular plate, and (2) from a differential strip to a rectangular plate with the former being in a plane that has parallel generating lines to the latter. This formula is then used to generate the view factors from a rectangular plate to some finite geometries via single integration.

[1]Professor, Department of Mechanical Engineering, The University of Akron, Akron, OH; Mem. ASME.

[2]Research Associate, Department of Mechanical Engineering, The University of Akron, Akron, OH 44325; Student Mem. ASME.

Contributed by the Heat Transfer Division for publication in the JOURNAL OF HEAT TRANSFER. Manuscript received by the Heat Transfer Division May 26, 1988. Keywords: Furnaces and Combustors, Radiation.

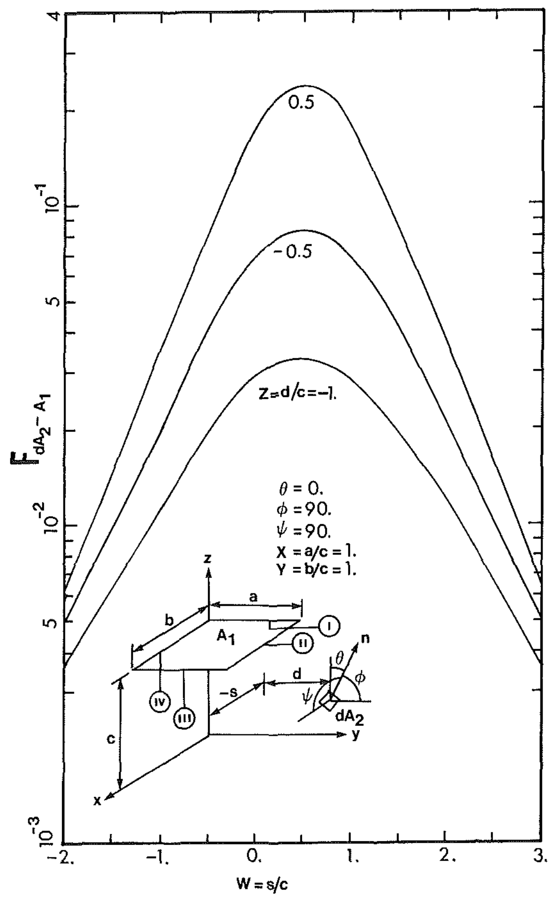

Fig. 1 Shape factor from a differential element to a rectangular plate

Mathematical Analysis and General Formulation

***(a)* Shape Factor From a Differential Element to a Nonintersecting Rectangle.** Consider an element with the coordinates and orientation shown in the sketch of Fig. 1, such that the plane of the differential element dA_2 does not intersect the plate. The view factor given by Sparrow and Cess (1978) has the form

$$F_{dA_2-A_1} = l_2/2\pi \oint [(z-z_2)dy-(y-y_2)dz)]/Le^2$$

$$+m_2/2\pi \oint [(x-x_2)dz-(z-z_2)dx]/Le^2$$

$$+n_2/2\pi \oint [((y-y_2)dx-(x-x_2)dy)]/Le^2$$

where the contour of integration consists of lines I to IV shown in the sketch; L_e is the distance from the element to the appropriate contour, $l_2 = \cos\Psi$, $m_2 = \cos\Phi$, and $n_2 = \cos\theta$. Performing the integration and nondimensionalizing the result yields

$$F_{dA_2-A_1} = \frac{l_2}{2\pi}\left\{\frac{1}{\sqrt{W^2+1}}\left(\tan^{-1}\frac{X-Z}{\sqrt{W^2+1}}+\tan^{-1}\frac{Z}{\sqrt{W^2+1}}\right)\right.$$

$$\left.-\frac{1}{\sqrt{1+(W-Y)^2}}\left(\tan^{-1}\frac{X-Z}{\sqrt{1+(W-Y)^2}}+\tan^{-1}\frac{Z}{\sqrt{1+(W-Y)^2}}\right)\right\}$$

$$+\frac{m_2}{2\pi}\left\{\frac{1}{\sqrt{1+Z^2}}\left(\tan^{-1}\frac{Y-W}{\sqrt{1+Z^2}}+\tan^{-1}\frac{W}{\sqrt{1+Z^2}}\right)\right.$$

$$\left.-\frac{1}{\sqrt{1+(Z-X)^2}}\left(\tan^{-1}\frac{Y-W}{\sqrt{1+(Z-X)^2}}\right)+\tan^{-1}\frac{W}{\sqrt{1+(Z-X)^2}}\right)\right\}$$

$$+\frac{n_2}{2\pi}\left\{\frac{W}{\sqrt{1+W^2}}\left(\tan^{-1}\frac{X-Z}{\sqrt{1+W^2}}+\tan^{-1}\frac{Z}{\sqrt{1+W^2}}\right)\right.$$